0273-2289/91/2829—0471$03.20

Metabolic Modeling of Fumaric Acid Production by *Rhizopus arrhizus*

IRENE C. GANGL,[1,4,*] WILLIAM A. WEIGAND,[2] AND FREDERICK A. KELLER[3]

[1]Department of Chemical Engineering, Illinois Institute of Technology, Chicago, IL 60616; [2]Department of Chemical and Nuclear Engineering, University of Maryland, College Park, MD 20742; [3]Cambridge BioScience Corporation, Massachusetts Biotech Research Park, 365 Plantation Street, Worcester, MA 01605; and [4]Present address: Allied-Signal, Inc., 50 East Algonquin Road, Box 5016, Des Plaines, IL 60017

ABSTRACT

A metabolic model is developed for fumaric acid production by *Rhizopus arrhizus*. The model describes the reaction network and the extents of reaction in terms of the concentrations of the measurable species. The proposed pathway consists of the Embden-Meyerhof pathway and two pathways to FA production, both of which require CO_2 fixation (the forward and the reverse TCA cycles). Relationships among the measurable quantities, in addition to those obtainable by a macroscopic mass balance, are found by invoking a pseudo-steady-state assumption on the nonaccumulating species in the pathway. Applications of the metabolic model, such as verifying the proposed pathway, obtaining the theoretical yield and selectivity, and detecting experimental errors, are discussed.

Index Entries: Fumaric acid; fermentation; metabolic modeling; *Rhizopus arrhizus*, CO_2 fixation.

INTRODUCTION

Fumaric acid has a variety of uses in the chemical, paper, food, and pharmaceutical industries (*1*). In 1978, 15% of the US production of fumaric acid was by microorganisms (2). One such organism is the fungus

*Author to whom all correspondence and reprint requests should be addressed.

Rhizopus arrhizus, which utilizes glucose, carbonate (from the neutralizing agent), and oxygen (from aeration for respiration) to produce fumaric acid, carbon dioxide, cell mass, and five other byproducts.

Several studies have used the concept of applying steady-state mass and energy balances to determine the most probable pathway for producing citric acid (*3–4*). Reardon et al. (*5*) were the first to apply this concept of metabolic modeling to batch fermentations by using stoichiometric relationships in the metabolic pathways to analyze pathway rates in anaerobic fermentations of *Clostridium acetobutylicum*. This approach, along with NAD(P)H fluorescence measurements, provided some insights on intracellular activities in both acidogenic and solventogenic cultures.

This study will develop a metabolic model that describes the reaction network and the extents of reaction in terms of the concentrations of the accumulating species. The extents of the individual reactions are found by taking the carbon and reductance-degree balances on all the species in the proposed pathway. The reductance-degree balance considers the number of available electrons, γ (nitrogen $= -3$, oxygen $= -2$, hydrogen $= +1$, carbon $= +4$). For example, the reductance degree of glucose ($C_6H_{12}O_6$) is 24 ($6\times4+12\times1+6\times[-2]$).

Either macroscopic or metabolic-model balances give the stoichiometric constraint that the overall reaction must satisfy at all times. Using Gibb's rule of stoichiometry, Tsai and Lee (*6*) show that the number of constraints given by the metabolic-model balance is always greater than or equal to the number given by the macroscopic balance. Only when the pathway method provides more constraints than the macroscopic method can one use the pathway method to determine the validity of a proposed reaction scheme. Knowledge of the correct pathway gives insight into how to control production at the enzyme level. Furthermore, an analysis of the pathway gives the maximum obtainable yield and selectivity.

Additional relationships among the measurable quantities are found by invoking a pseudo-steady-state (pss) assumption on the nonaccumulating species in the pathway. These relationships are equivalent in function to the "fermentation equations" that Papoutsakis (*7–9*) derived for various anaerobic fermentations. Both the fermentation equations and the pss equations give the stoichiometric relationship among the substrate and the products (including biomass) in terms of molar extents of reaction, and may be used (a) to determine the maximum possible yield and selectivity for each fermentation product, (b) to determine errors in a set of experimental data, and (c) as a gateway sensor for calculating concentrations of fermentation products, which cannot be measured directly.

MATERIALS AND METHODS

The fermentations were conducted with *Rhizopus arrhizus* NRRL 2582 in a 2-L computer-controlled fermenter (Queue Systems, ZMS-7000,

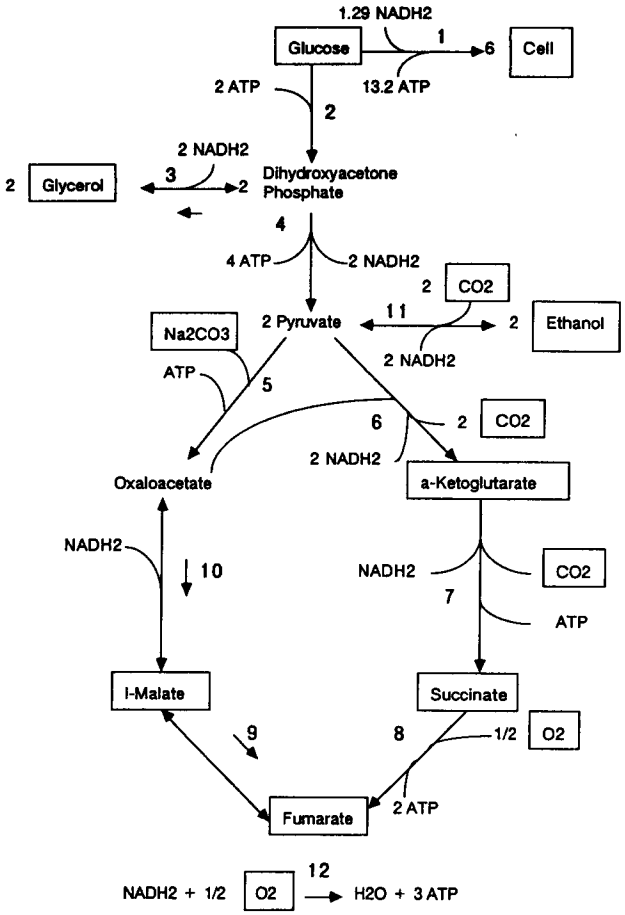

Fig. 1. Proposed metabolic pathway for FA production.

Parkersburg, WV). A 15% (w/v) solution of sodium carbonate (Na_2CO_3) was added on demand during the fermentation to neutralize the broth. The fermentation medium was limited by ammonium sulfate, and glucose served as the primary carbon substrate. The composition of the media, details of the equipment used, and analytical techniques employed are given elsewhere (*10*). Glycerol, ethanol, fumaric acid, l-malic acid, α-ketoglutaric acid, and succinic acid were all quantified with the high-performance liquid chromatography system previously described (*10*). The exit gas was analyzed for CO_2 and O_2 with a mass spectrometer (Perkin Elmer, #1200, Tinton Falls, NJ).

PROPOSED PATHWAY

The proposed pathway to product production in *R. arrhizus* consists of the Embden-Meyerhof pathway and two pathways to fumaric acid production, the forward and the reverse TCA cycles (based on *11–13, see* Fig. 1).

Both cycles share a common CO_2-fixing step (Reaction 5). For simplicity, the oxidized forms of $NADH_2$ and ATP have been omitted in the figure, and only the balanced carbon is shown. The boxed species are the products, which accumulate and are measured analytically. Because all reactions shown in Fig. 1 are linearly independent, none of the reactions can be represented as a linear combination (or sum) of the other reactions. To obtain linearly independent reactions, some reactions (such as Reaction 12, representing the respiratory chain) were found by summing several intermediate reactions. The formula for the cell mass is taken as $CH_{1.76}O_{0.47}N_{0.13}$ (based on cell-composition data of a 47-h culture—*see 14*). The yield of cell mass from ATP in Reaction 1 is taken as $Y_{ATP}=10.5$ g cell/mol ATP (*15*). The coefficient of $NADH_2$ in Reaction 1 is found by balancing the hydrogen atoms as follows:

$$\text{glucose } (C_6H_{12}O_6) + 1.29(NADH_2) + 0.78(NH_3) \rightarrow 6\,\text{cell}(CH_{1.76}O_{0.47}N_{0.13}) + 3.18(H_2O) \quad (1)$$

In the TCA cycle, 1 mol of succinate forms 1 mol of fumarate plus 1 mol of $FADH_2$. One mole of $FADH_2$ is oxidized in the respiratory chain reactions to form 2 mol of ATP. Assuming $FADH_2$ does not accumulate in the cells, Reaction 8 of the pathway represents the sum of the TCA cycle and the respiratory chain reactions. Accumulation of ATP inside the cells is associated with fermentations starting with high glucose concentrations, such as the citric acid fermentation (*3*). Because of the expected excess ATP production, Verhoff and Spradlin (*3*) suggest that Reaction 12 may be rewritten as

$$NADH_2 + (1/2)O_2 \rightarrow H_2O \quad (2)$$

The fungus will still consume oxygen to oxidize $NADH_2$ in the cytochrome electron chain, but will generate little ATP. Because of the possibility of Eq. 2, an ATP balance will not be considered in the following analysis. Therefore, the pathway has 12 reactions and 15 species.

One immediate use of the proposed pathway is to determine the maximum possible yield and selectivity of fumaric acid. Table 1 shows the results of summing the reactions of the reverse and the forward TCA cycles. To maximize the carbon available to fumaric acid and thereby maximize yields, cell growth is neglected, and the sole products are assumed to be fumaric acid and CO_2. Both pathways give a maximum selectivity of 100%. The reverse (or reductive) TCA cycle produces no byproducts and therefore is very efficient, giving a 200% molar yield of fumarate. The forward TCA (or oxidative) cycle, on the other hand, produces 3 mol of CO_2, energy (in the form of ATP or GTP), and reducing power (in the form of $NADH_2$ or $FADH_2$), resulting in only a 100% molar yield. The most significant insight from this analysis is that both the forward and the reverse TCA cycles require the fixation of 1 mol of CO_2 for every mole of fumarate produced. By Reaction 5, the source of this CO_2 is the neutralizing agent

Table 1
Net Reactions Producing Fumaric Acid

I. Reverse TCA Cycle*

2) $GLU + 2ATP \rightarrow 2DHP$

4) $2DHP \rightarrow 2PYR + 4ATP + 2NADH_2$

5) $2PYR + 2Na_2CO_3 + 2ATP \rightarrow 2OXAL$

10) $2OXAL + 2NADH_2 \rightarrow 2MA$

9) $2MA \leftrightarrow 2FA$

Net: $GLU + 2Na_2CO_3 \rightarrow 2FA$

II. Forward TCA Cycle*

2) $GLU + 2ATP \rightarrow 2DHP$

4) $2DHP \rightarrow 2PYR + 4ATP + 2NADH_2$

5) $PYR + Na_2CO_3 + ATP \rightarrow OXAL$

6) $PYR + OXAL \rightarrow \alpha KA + 2CO_2 + 2NADH_2$

7) $\alpha KA \rightarrow SA + CO_2 + GTP + NADH_2$

8) $SA \rightarrow FA + FADH_2$

Net: $GLU + Na_2CO_3 \rightarrow FA + 3CO_2 + (ATP + GTP) + (5NADH_2 + FADH_2)$

*GLU=glucose, DHP=dihydroxyacetone phosphate, PYR=pyruvate, OXAL=oxaloacetate, MA=l-malate, FA=fumarate, αKA=α-ketoglutarate, SA=succinate.

(either Na_2CO_3 or $CaCO_3$). Using labeled $NaH^{14}CO_3$, Kenealy et al. (*12*) experimentally determined that the fungus fixes the labeled carbon from the base into the fumarate product.

DERIVATION

A mass balance over the fermentor gives us the following equation (*16*).

$$\begin{matrix}\text{(accumulation)} & = & \text{(conversion)} & + & \text{(in-out transport)} \\ d\,\mathbf{C}\,/\,dt & = & \mathbf{R}_a & + & \Phi\end{matrix} \qquad (3)$$

where t = time (h), $\mathbf{C}$ = vector of concentrations of chemical compounds (mol/L), $\mathbf{R}_a$ = vector of net production rates of each of the compounds in the system (mol/L/h), and Φ = vector of net rates of transport (mol/L/h).

The only compounds transported into or out of the system are O_2, CO_2, and the base. Rather than considering the actual concentration of these three compounds in the broth, we can define the system to include the total CO_2, O_2, and base produced (or consumed). Volume changes caused by base additions can be corrected by multiplying the measured accumulation of each compound by the ratio of the actual fermenter volume to the calculated fermenter volume without dilution. The defined system is a batch process for which

$$\Phi = 0 \tag{4}$$

Therefore, by Eqs. 3 and 4

$$d\mathbf{C} / dt = \mathbf{R}_a \tag{5}$$

However,

$$\mathbf{R}_a = x\,\alpha\,\mathbf{V} \tag{6}$$

where x = concentraiton of dry cell mass (g/L), α = stoichiometric matrix (mol/mol), and $\mathbf{V}$ = vector of specific rates of reaction (mol/g cell/h).

Equation 6 states that the net production rate of a compound is equal to the sum of the rates of reaction producing or consuming the compound. Substituting Eq. 6 into Eq. 5, we obtain

$$d\,\mathbf{C} / dt = x\,\alpha\,\mathbf{V} \tag{7}$$

Equation 7 represents the carbon and reductance degree balances that make up the metabolic model.

Determining the time derivatives of the measured concentration profiles (left-hand side of Eq. 7) would require numerical differentiation, which is subject to large errors (*17,18*). To reduce numerical errors in this analysis and eliminate possible bias introduced into the data from a spline-smoothing procedure, the extents (mol/L) of reaction, rather than the reaction rates, were calculated. The extent of reaction is a measure of the progress of a reaction, independent of the stoichiometric coefficients. The conversion differs from the extent in that it represents the fraction of reactant that reacts, and it depends on the reactant chosen. The relationship between the extent of reaction and the specific reaction rate is as follows:

$$x\,\mathbf{V} = d\,\mathbf{E} / dt \tag{8}$$

where $\mathbf{E}$ = vector of extents or reaction (mol/L).

Substituting Eq. 7 into Eq. 8, we obtain

$$d\,\mathbf{C} / dt = \alpha\,d\,\mathbf{E} / dt \tag{9}$$

Integrating Eq. 9 over time and setting the initial values of the extents to zero gives:

$$(\mathbf{C} - \mathbf{C}_0) = \alpha\,\mathbf{E} \tag{10}$$

where $\mathbf{C}_0$ = vector of initial concentrations of chemical compounds (mol/L).

Table 2
Balances from the Proposed Pathway

glucose	$C_g - C_{g0}$		-1/6	-1/2	0	0	0	0	0	0	0	0	E_1
cell	$C_x - C_{x0}$		1	0	0	0	0	0	0	0	0	0	E_2
glycerol	$C_y - C_{y0}$		0	0	1	0	0	0	0	0	0	0	E_3
CO_2	$C_c - C_{c0}$		0	0	0	0	2	1	0	0	0	1	0	E_5
α-ketoglutarate	$C_k - C_{k0}$		0	0	0	0	1	-1	0	0	0	0	0	E_6
succinate	$C_s - C_{s0}$	= x	0	0	0	0	0	1	-1	0	0	0	0	E_7
fumarate	$C_f - C_{f0}$		0	0	0	0	0	0	1	1	0	0	0	E_8
l-malate	$C_m - C_{m0}$		0	0	0	0	0	0	0	-1	1	0	0	E_9
ethanol	$C_e - C_{e0}$		0	0	0	0	0	0	0	0	0	1	0	E_{10}
base	$C_b - C_{b0}$		0	0	0	-1	0	0	0	0	0	0	0	E_{11}
O_2	$C_o - C_{o0}$		0	0	0	0	0	0	-1/2	0	0	0	-1/2	E_{12}

The pseudo-steady-state equations:

dihydroxyacetone phosphate	$E_2 = E_3 + E_4$
pyruvate	$E_4 = E_5 + E_6 + E_{11}$
oxaloacetate	$E_5 = E_6 + E_{10}$
$NADH_2$	$0.215\,E_1 + E_3 + E_{10} + E_{11} + E_{12} = E_4 + 2\,E_6 + E_7$

No significant amounts of dihydroxyacetone phosphate (DHP), pyruvate, oxaloacetate, and $NADH_2$ accumulate outside the cells. The pss assumption states that, relative to the measurable quantities, the accumulation of these metabolic intermediates can be taken as zero. Reardon et al. (*5*) apply this concept to the metabolic intermediates in their proposed pathway for a batch fermentation of *Clostridia*.

Table 2 gives the results of apply Eq. 10 to the proposed pathway. The matrix in Table 2 can be solved for 11 of the 12 extents of reaction by inverting the stoichiometric matrix α. Because there are 12 reactions, but only 11 accumulating species, one of the pss equations (the DHP balance) is required to solve for the twelfth extent. Table 3 gives the solution of the extents of reaction in terms of the accumulating concentrations.

The remaining pss equations in Table 2 provide three additional relationships (the pyruvate, oxaloacetate, and $NADH_2$ balances). Substituting the solutions of the extents into the pss equations and rearranging, we obtain

Table 3
The Solution of the Extents of Reaction for the Proposed Pathway

$$E_1 = C_x - C_{x0}$$

$$E_2 = -(1/3)(C_x - C_{x0}) - 2(C_g - C_{g0})$$

$$E_3 = (C_y - C_{y0})$$

$$E_4 = -(1/3)(C_x - C_{x0}) - 2(C_g - C_{g0}) - (C_y - C_{y0})$$

$$E_5 = -(C_b - C_{b0})$$

$$E_6 = (1/3)(C_c - C_{c0}) + (1/3)(C_k - C_{k0}) - (1/3)(C_e - C_{e0})$$

$$E_7 = (1/3)(C_c - C_{c0}) - (1/3)(C_e - C_{e0}) - (2/3)(C_k - C_{k0})$$

$$E_8 = (1/3)(C_c - C_{c0}) - (1/3)(C_e - C_{e0}) - (2/3)(C_k - C_{k0}) - (C_s - C_{s0})$$

$$E_9 = -(1/3)(C_c - C_{c0}) + (1/3)(C_e - C_{e0}) + (2/3)(C_k - C_{k0}) + (C_s - C_{s0}) + (C_f - C_{f0})$$

$$E_{10} = -(1/3)(C_c - C_{c0}) + (1/3)(C_e - C_{e0}) + (2/3)(C_k - C_{k0}) + (C_s - C_{s0}) + (C_f - C_{f0}) + (C_m - C_{m0})$$

$$E_{11} = (C_e - C_{e0})$$

$$E_{12} = -2(C_o - C_{o0}) - (1/3)(C_c - C_{c0}) + (1/3)(C_e - C_{e0}) + (2/3)(C_k - C_{k0}) + (C_s - C_{s0})$$

$$-\{6(C_g - C_{g0}) + (C_b - C_{b0})\} = 4(C_f - C_{f0}) + 4(C_m - C_{m0}) + 4(C_s - C_{s0}) + 5(C_k - C_{k0}) + 3(C_y - C_{y0}) + 2(C_e - C_{e0}) + (C_x - C_{x0}) + (C_c - C_{c0}) \quad (11)$$

$$-(C_b - C_{b0}) = (C_f - C_{f0}) + (C_m - C_{m0}) + (C_k - C_{k0}) + (C_s - C_{s0}) \quad (12)$$

$$4(C_o - C_{o0}) = 4.43(C_x - C_{x0}) + 14(C_y - C_{y0}) + 12(C_e - C_{e0}) + 16(C_k - C_{k0}) + 14(C_s - C_{s0}) + 12(C_f - C_{f0}) + 12(C_m - C_{m0}) + 24(C_g - C_{g0}) \quad (13)$$

(For definitions of subscripts, *see* Table 2.) Equation 11 is the overall carbon balance, with both glucose and the neutralizing agent serving as the carbon substrates. A macroscopic balance gives only the overall balances on carbon (Eq. 11) and reductance degree (Eq. 13). The additional relationship given by the metabolic-pathway mass balance is Eq. 12, a titration equation, which states that the amount of base neutralized is equal to the total acid produced. The net pathway analysis (Table 1) suggests that the fungus must fix 1 mol of base for every mole of acid produced. In the fermentation broth, CO_2 from glucose metabolism is indistinguishable from CO_2 derived from base dissolution. Therefore, the proposed pathway requires that an *amount* equal to the carbon contained in the neutralizing agent is fixed into the TCA cycle; no additional metabolic CO_2 is necessary for fumaric acid production.

MODEL VERIFICATION

The three pss equations allow us to verify the model by giving the system three degrees of freedom. This means that, out of the eleven measurements (boxed species in Fig. 1), we only need eight (11–3) measurements to describe the entire system. After rearranging and setting the initial concentrations to zero, the three pss equations, 11–13, become

$$C_f = (1/3)(C_o - C_{o0}) - 0.3692(C_x - C_{x0}) - (7/6)(C_y - C_{y0} + C_s - C_{s0}) - (C_e - C_{e0} + C_m - C_{m0}) - (4/3)(C_k - C_{k0}) - 2(C_g - C_{g0}) \quad (14)$$

$$C_c = 0.1075(C_x - C_{x0}) + (1/2)(C_s - C_{s0} + C_y - C_{y0}) + (C_e - C_{e0}) - (C_o - C_{o0}) \quad (15)$$

$$C_b = -(1/3)(C_o - C_{o0}) + 0.3692(C_x - C_{x0}) + (7/6)(C_y - C_{y0}) + (1/6)(C_s - C_{s0}) + (C_e - C_{e0}) + (1/3)(C_k - C_{k0}) + 2(C_g - C_{g0}) \quad (16)$$

Figure 2 shows the measured and predicted profiles (Eqs. 14–16) of fumaric acid (FA), CO_2, and Na_2CO_3 for experiment M20, conducted at pH 5.5. The solid lines predicted by the metabolic model are in good agreement with the experimental data points (marked by the symbols). The predicted FA profile deviates from the measured values during 40–60 h and after 110 h, giving a 10.5% difference by the end of the fermentation. However, the experimental base profile does not increase in response to the increased acidity of the high FA measurements. This indicates that the experimental measurements of FA at those points, not the model, is in error.

The three pss equations may be used to detect experimental errors. Rearranging Eq. 14 and setting C_{o0} to zero gives

$$C_o = 1.1075(C_x - C_{x0}) + 3.5(C_y - C_{y0}) + (C_s - C_{s0}) + 6(C_g - C_{g0}) + 3(C_f + C_e - C_{e0} + C_m - C_{m0}) + 4(C_k - C_{k0}) \quad (17)$$

Substituting Eq. 17 into Eq. 15, we obtain

$$C_c = -6(C_g - C_{g0}) - (C_x - C_{x0}) - 4(C_k - C_{k0}) - 2(C_e - C_{e0}) - 3(C_y - C_{y0} + C_f + C_m - C_{m0} + C_s - C_{s0}) \quad (18)$$

Figure 3 gives the base, O_2, and CO_2 profiles predicted by Eqs. 12, 17, and 18 for experiment M21 conducted at pH 6.0. The predicted base and CO_2 profiles are in good agreement with the experimental data. but the measured O_2 profile is much lower than predicted throughout most of the run. Because of an air leak, the flow rate of the exit gas was low. Therefore, the mass spectrometer may not have been able to give accurate readings of the exit-gas stream. The model can be used to obtain an estimate of the actual O_2 profile.

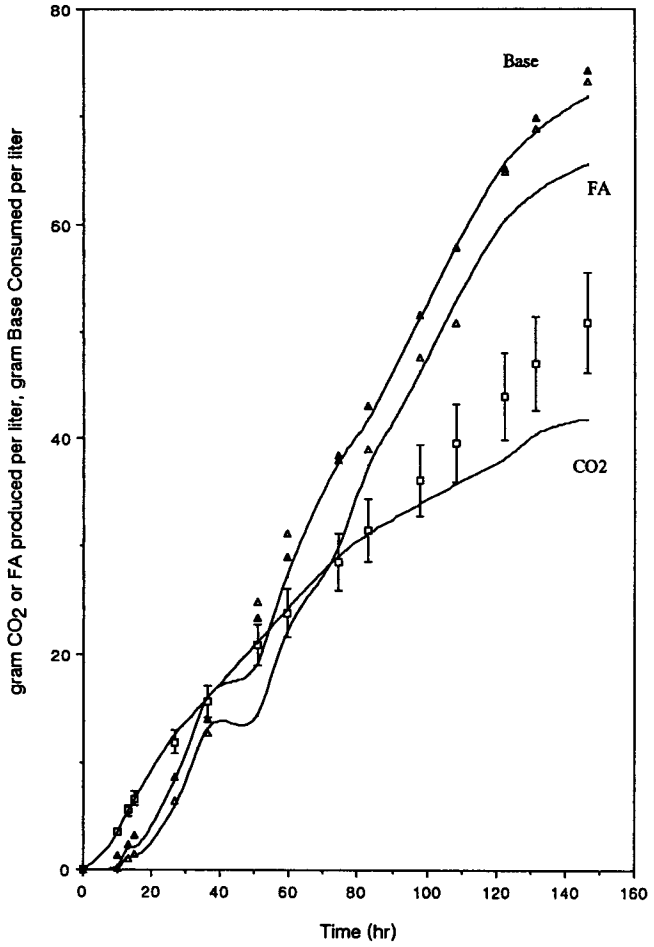

Fig. 2. Predicted and measured profiles for M20: ____, predicted profile; ▲——▲, Na_2CO_3 added; △——△, FA; □——□, carbon dioxide.

One may test the pss assumption by plotting the concentration profile of one of the nonaccumulating species. For example, based on Fig. 1, the concentration of $NADH_2$ may be written in terms of extents:

$$C_n = -0.215\,E_1 - E_3 + E_4 + 2\,E_6 + E_7 - E_{10} - E_{11} - E_{12} \qquad (19)$$

where C_n = concentration of $NADH_2$ (mol/L) and E_j = extent of reaction j (mol/L). Substituting the solution of the extents given in Table 3 into Eq. 19 gives

$$\begin{aligned} C_n = {} & -0.5483\,(C_x - C_{x0}) - 2\,(C_y - C_{y0}) - 2\,(C_g - C_{g0}) + (5/3)\,(C_c - C_{c0}) \\ & - (4/3)\,(C_k - C_{k0}) - (8/3)\,(C_e - C_{e0}) - 2\,(C_s - C_{s0}) - (C_f - C_{f0}) \\ & - (C_m - C_{m0}) + 2\,(C_o - C_{o0}) \end{aligned} \qquad (20)$$

Since $NADH_2$ is associated with the cell mass, the specific $NADH_2$ profile is considered:

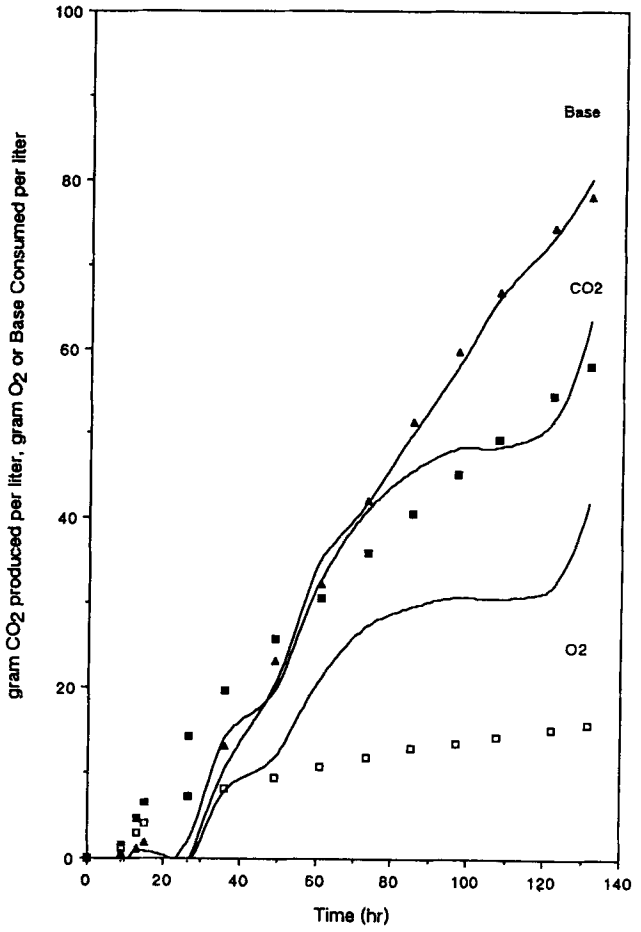

Fig. 3. Predicted and measured gas profiles for M21: ____, predicted profile; ▲——▲, Na_2CO_3 added; ■——■, carbon dioxide; □——□, oxygen.

$$\eta = C_n / C_x \quad (21)$$

where η = specific $NADH_2$ concentration (mol/g cell).

The pss assumption predicts the specific $NADH_2$ profile will be zero throughout the fermentation. Using a corrected oxygen profile based on Fig. 3, the specific $NADH_2$ profile of M21 is within the pss assumption throughout the fermentation (*see* Fig. 4).

RESULTING PROFILES

Table 4 summarizes the experiments used in this analysis. Figure 5 plots the extents of the reactions producing or consuming pyruvate, a key intermediate (*see* Fig. 1), vs the amount of glucose consumed. The extent of reaction for the Embden-Meyerhof (EM) pathway producing pyruvate (Reaction 4) is linearly related to the amount of glucose consumed. Differ-

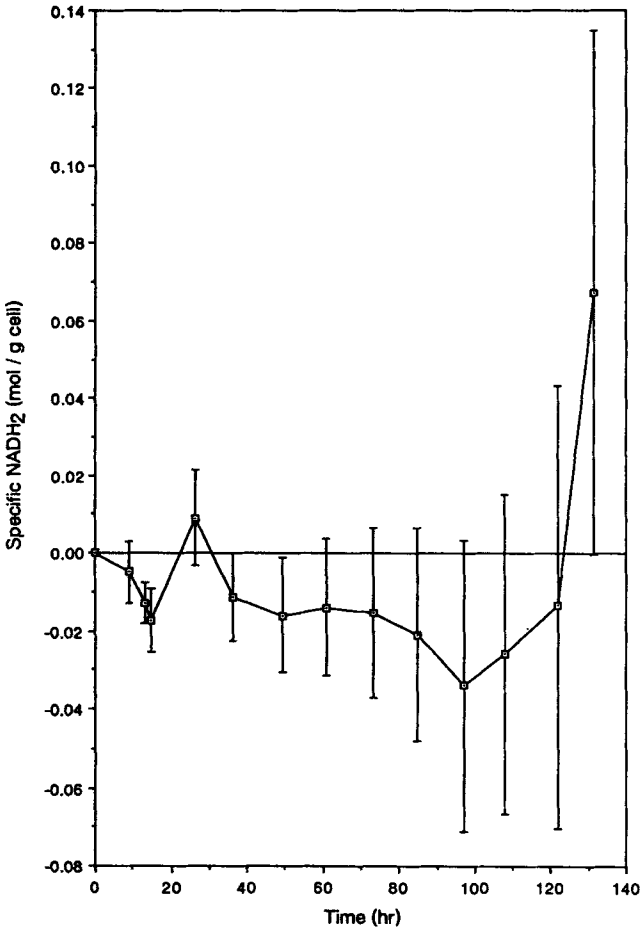

Fig. 4. The specific $NADH_2$ profile for M21.

ences in the extents of Reaction 1 (cell production) and Reaction 3 (glycerol production) do not change the extent of glucose utilization in the EM pathway, probably because these extents are very small compared to the EM pathway extent. The slope of the extent 4 plot is 1.87 ± 0.02 mol through the EM pathway per mole of glucose consumed. If all the available glucose were to enter the EM pathway, this slope would be equal to 2. Therefore, regardless of pH, the cells convert a constant 93.5% ($[1.87/2] \times 100$) of the glucose to pyruvate. Because the precursor of ethanol production is pyruvate (Reaction 11), not all of this pyruvate is available to the TCA cycle for acid production. Figure 5 shows that the yield of ethanol from glucose is slightly higher for the pH 6.0 fermentation, than for the pH 5.5 fermentation, and the extent of CO_2 fixation is slightly lower, although both fermentations have the same extent of the forward TCA cycle (Reaction 6, *see* Fig. 5). Therefore, less carbon is available to the more efficient reverse TCA cycle in the pH 6.0 fermentation, resulting in a lower overall efficiency yield of total acids (53 wt% at pH 6.0 vs 72 wt% at pH 5.5).

Table 4
Summary of Experiments Used in the Metabolic Modeling Analysis

	M20	M21
Methanol (%, v/v)	1.5	1.5
Base	Na_2CO_3	Na_2CO_3
pH	5.5	6.0
Initial glucose concentration (g/l)	102	120
Carbon/nitrogen (g/g)	134	203
Morphology (F=filamentous)	F	F
Max fumaric acid concentration (g/l)	73.3	61.6
Max malic acid concentration (g/l)	7.22	18.2
Efficiency yield of fumaric acid (%, g FA/g GLU)	72	53
Efficiency yield of total acids (%, g TA/g GLU)	87	74
Overall fumaric acid productivity (g/l/hr)	0.50	0.51
Overall total acid productivity (g/l/hr)	0.60	0.71
Selectivity (%, g FA/g TA)	83	71
Overall glucose uptake (g/l/hr)	0.70	0.95

The average amount of CO_2 fixed per glucose consumed is constant at 1.2 mol/mol (Reaction 5, *see* Fig. 5). The amount of carbonate the fungus fixes from the neutralizing agent is equal to the total acids produced (Table 1). Therefore, the model predicts an efficiency yield of 1.2 mol of total acids per mole of glucose consumed over a wide range of conditions. The range of experimental total-acid yields encompasses the calculated value (1.23 ± 0.09 mol/mol).

Figure 6 profiles the ratio of FA produced by the reverse TCA cycle to FA produced by the forward TCA cycle ($R_f = E_9/E_8$). The negative values

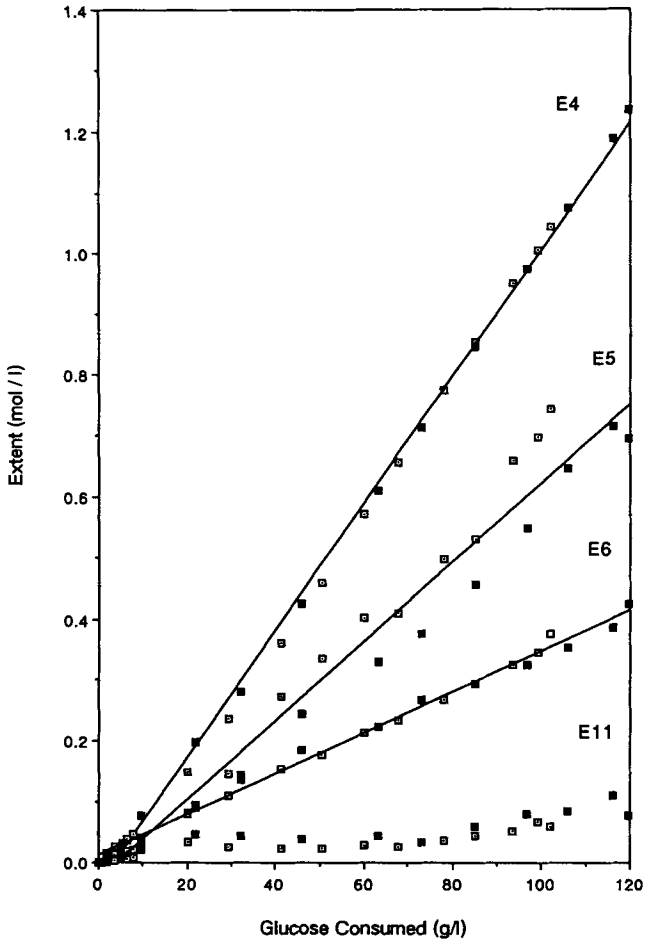

Fig. 5. The extents of reactions producing or consuming pyruvate: □——□, M20; ■——■, M21.

during the growth cycle (< 20 h) are caused by the negative values of the extent of the reverse TCA cycle. This indicates that only the forward TCA cycle operates during the growth phase. Because most points fall below one, fumaric acid is produced primarily from the forward TCA cycle. The experiment conducted at pH 5.5 (M20) has higher R_f values than the experiment conducted at pH 6.0 (M21) because, compared to M21, M20 has a higher selectivity, by virtue of the higher extent of reaction 9, and a higher efficiency yield (*see* Table 4).

CONCLUSIONS

The metabolic model developed here describing FA production by *Rhizopus arrhizus* is essentially a macroscopic mass balance on a proposed pathway. The model cannot be used to predict results at new conditions.

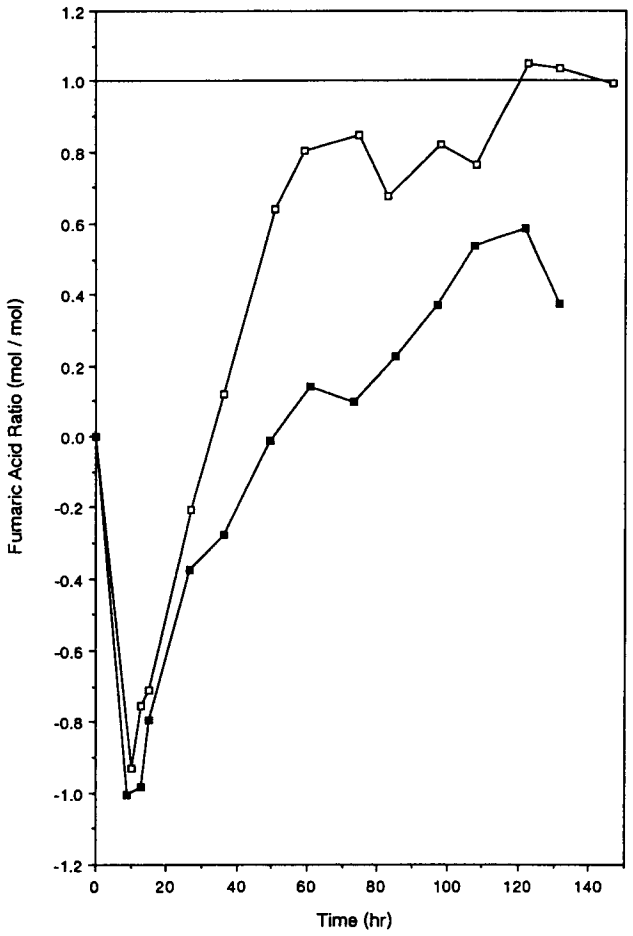

Fig. 6. Profiles of the ratio of FA produced via the forward TCA cycle to that produced via the reverse TCA cycle: □——□, M20; ■——■, M21.

Rather, the model describes the relationships among the measurable quantities, which enables one to better examine the data and to determine experimental consistency. The metabolic pathway proposed in Fig. 1 fits the experimental data. This analysis reveals that, regardless of the pathway to FA production, the fungus fixes 1 mol of CO_2 for every mole of FA produced. The amount fixed is equal to the CO_2 contained in the added neutralizing agent ($CaCO_3$ or Na_2CO_3). Kenealy et al. (*12*) have experimentally determined that the enzymes of the reverse TCA cycle are active in *R. arrhizus*. As seen in Fig. 6, the model shows that the forward TCA cycle operates exclusively during the growth phase, and that both the forward and the reverse TCA cycles operate simultaneously during the acid-production phase. Therefore, the metabolic model may be used before undertaking tedious enzyme studies to screen and test possible pathways. The model is also useful for detecting errors in the experimental data, such as an erroneously low O_2 measurement caused by an air leak.

An analysis of the extent of reaction reveals that FA is produced primarily from the forward TCA cycle (*see* Fig. 6), with the pH 5.5 fermentation giving a higher ratio of FA produced from the reverse TCA cycle than the pH 6.0 fermentation. A higher extent of the reverse TCA cycle would give higher efficiency yields of FA from glucose.

ACKNOWLEDGMENT

We would like to express our gratitude to Corn Products, Inc. (Summit-Argo, IL), who initially supported this work, in addition to allowing F. K. a 2-yr leave of absence to teach at IIT and granting I. G. a fellowship; and to acknowledge the continued support provided by the Amoco Foundation's Grant #254.

REFERENCES

1. Robinson, W. D. and Mount, R. A. (1981), *Kirk-Othmer Encyclopedia of Chemical Technology*, vol. 14, Grayson, M., and Eckroth, D., eds., Wiley, New York, p. 770–793.
2. Sinskey, A. J. (1983), *Organic Chemicals from Biomass*, Wise, D. L., ed., Benjamin/Cummings, London, p. 1–67.
3. Verhoff, F. H. and Spradlin, J. E. (1976), *Biotech. Bioeng.* **18,** 425–433.
4. Aiba, S. and Matsuoka, M. (1979), *Biotechnol. Bioeng.* **21,** 1373–1386.
5. Reardon, K. F., Scheper, T.-H., and Bailey, J. E. (1987), *Biotechnol. Prog.* **3,** 153–167.
6. Tsai, S. P. and Lee, Y. H. (1988), *Biotechnol. Prog.* **4,** 82–88.
7. Papoutsakis, E. T. (1984), *Biotechnol. Bioeng.* **26,** 174–187.
8. Papoutsakis, E. T. and Meyer, C. L. (1985), *Biotechnol. Bioeng.* **27,** 50–60.
9. Papoutsakis, E. T. and Meyer, C. L. (1985), *Biotechnol. Bioeng.* **27,** 67–80.
10. Gangl, I. C., Weigand, W. A., and Keller, F. A. (1990), *Appl. Biochem. Biotechnol.* **24/25,** 663–677.
11. Bailey, J. E. and Ollis, D. F. (1986), *Biochemical Engineering Fundamentals*, 2nd Ed., (McGraw-Hill, New York), 802–815.
12. Kenealy, W., Zaady, E., Du Preez, J. C., Steiglitz, B., and Goldberg, I. (1986), *Appl. Environ. Microbiol.* **52,** 128–133.
13. Rawn, J. D. (1983), *Biochemistry*, Harper & Row, New York, p. 553–606.
14. Gangl, I. C. (1990), Modeling and Economics of Fumaric Acid Production by *Rhizopus arrhizus*, PhD thesis, Illinois Institute of Technology, Chicago, IL.
15. Wang, D. I. C., Cooney, C. L., Demain, A. L., Dunnill, P., Humphrey, A. E., and Lilly, M. D. (1979), *Fermentation and Enzyme Technology*, Wiley, New York, p. 76.
16. Roels, J. A. (1978), *Proc. 1st Eur. Cong. Biotechnol.* 1978, part 3, Verlag Chemie, Weinheim, FRG, p. 221–249.
17. Forsythe, G. E., Malcolm, M. A., and Moler, C. B. (1977), *Computer Methods for Mathematical Computations*, Prentice Hall, Englewood Cliffs, NJ, p. 84.
18. Pollard, J. H. (1977), *A Handbook of Numerical and Statistical Techniques*, Cambridge University Press, Cambridge, UK, chapter 6.